MicroRNA-based cancer mortality risk scoring system and hTERT expression linked with risk-adjusted treatment strategy in early-stage oral squamous cell carcinoma

Angela J. Yoon[1], Regina M. Santella[2], Shuang Wang[2], David I. Kutler[3], Richard D. Carvajal[1], Elizabeth Philipone[1], Tian Wang[2], Scott M. Peters[1], Claire R. Stewart[3], Fatemeh Momen-Heravi[1], Scott Troob[1], Matt Levin[4], Zohreh AkhavanAghdam[4], Austin J. Shackelford[1], Carleigh R. Canterbury[1], Masataka Shimonosono[1] and Hiroshi Nakagawa[1]

Author's Affiliations: [1]Columbia University Irving Medical Center, New York, NY, USA; [2]Columbia University Mailman School of Public Health, New York, NY, USA; [3]Weill Cornell Medicine, New York, NY, USA; [4]Cell IDx, San Diego, CA, USA.

Corresponding Author: Angela J. Yoon, Division of Oral and Maxillofacial Pathology, Columbia University Irving Medical Center, 630 West 168th Street, PH15W-1562, New York, NY 10032. Phone: 212-305-7676; E-mail: ajk55@cumc.columbia.edu

ABSTRACT

We have developed and validated a novel microRNA (miRNA)-based prognostic model to predict survival outcome in oral squamous cell carcinoma (OSCC) patients who are already categorized into 'early-stage' by the TNM system. A total of 836 early-stage OSCC patients were assigned the mortality risk scores. We evaluated the efficacy of various treatment regimens in terms of survival benefit compared to surgery only in patients stratified into high and low mortality risk categories. Within the high-risk group, surgery with neck dissection significantly improved the 5-year survival to 75% from 46% ($p<0.001$) with surgery only. A Cox proportional hazard model on time-to-death suggests a hazard ratio of 0.37 comparing surgery with neck dissection to surgery only (95% CI: 0.2-0.6; $p=0.0005$). For the low-risk group, surgery only without neck dissection is the most beneficial treatment modality, as opposed to the high-risk group, in which surgery with neck dissection significantly improves 5-year survival. Regardless of treatment selected, those with risk score ≥ 1 may benefit from additional therapy to prevent cancer relapse. Based on functional analysis of the prognostic miRNAs, we identified hTERT (human telomerase reverse transcriptase) as a promising drug target to prevent cancer relapse, thereby improving cancer-free survival. We also established a functional platform for patient-derived organoid-based drug testing in an effort to link prognostic marker-based mortality risk assessment with appropriate risk-adjusted therapy to improve overall survival.

INTRODUCTION

An estimated 49,000 people in United States are diagnosed with oral squamous cell carcinoma (OSCC) each year [1,2]. Leading etiologic factors include tobacco and alcohol [1-5]. While 80% of oropharyngeal cancers are related to high-risk human papillomavirus (HPV types 16 and 18), the incidence of high-risk HPV-related oral cancer is relatively low, estimated to be ~4% [4,5]. Despite advances in cancer diagnosis and treatment, the overall 5-year survival rate for OSCC remains the lowest among malignancies and, in fact, has been <50% for the last three decades [1-5].

Among newly diagnosed oral cancer cases, ~80% are in the tumor-node-metastasis (TNM) Stage I/II without regional lymph node involvement or distant metastasis [3]. Hence, a window of opportunity exists in which accurate prognostication and subsequent decisions for appropriate treatment could dramatically improve 5-year survival of patients with this deadly disease.

While the TNM stage is considered the key prognostic determinant in oral cancer [6], it is incapable of delineating individual risk for patients within the same TNM stage strata. To address these critical gaps, we performed next generation sequencing to identify microRNA (miRNA) signatures highly prognostic of cancer-specific mortality risk [7]. microRNAs are small, 18-24 nucleotide long, non-coding RNA molecules that regulate the expression of targeted genes either by facilitating mRNA degradation or by repressing translation [8,9]. One miRNA is capable of binding over 100 different mRNAs with different binding efficiencies and plays a crucial role in their post-transcriptional regulation [8-12]. microRNAs control cell growth, apoptosis and differentiation, and various types of cancer have demonstrated distinct miRNA expression profiles [8-12]. Thus far, a number of miRNAs associated with clinical outcomes have been reported for lung, breast, gastric and pancreatic cancers, as well as OSCC/head and neck carcinomas [12-14].

In the prognostic model, we included pertinent clinico-demographic covariates [7]. Therefore, the final prognostic model was built based on both expression of the miRNAs (miRNA-127-3p, 4736, 655-3p) and clinico-demographic covariates (TNM Stage I vs II, histologic grade well vs moderate/poor), which allowed for multiple risk factors to be used systematically and reproducibly to maximize the prognostic power. The prognostic model was subjected to rigorous internal validation, followed by external validation, which included patient populations from Pennsylvania, Iowa and Hawaii [7]. The performance of the model, in terms of its discriminatory power to differentiate between high and low cancer-specific mortality risk was meticulously verified. The area under the curve (AUC) of the receiver operating characteristic (ROC) curve with the miRNA-based 5-plex marker panel was 0.83 ($p<0.001$), 0.87 ($p<0.001$) and 0.81 ($p<0.001$) in internal test, internal validation and external validation cohorts, respectively, demonstrating uniformly significant prognostic value [7].

From the final prognostic model, we constructed a robust mortality risk score formula. This personalized formula consisted of the patient's miRNA expression levels and prognostic covariates weighed by their regression coefficient. The main purpose of the risk score formula is for clinicians to easily translate miRNA levels obtained from the clinical laboratory, along with known clinico-demographic variables into the patient's risk scores, which will serve as a practical method to assess patient-specific mortality risk in the clinical setting. The risk score from the 5-plex marker panel consisting of miRNAs-127-3p, 4736, 655-3p, TNM stage and histologic grading stratified patients initially into high (≥ 0) vs low (<0) risk categories, and then sub-risk stratified into finer risk categories [highest (risk score ≥ 2) vs moderately-high (risk score 1-2) vs moderately-low (risk score 0-1) vs low risks (risk score <0)]. Compared to the low-risk strata (<0), the highest-risk strata (≥ 2) had 23-fold increased mortality risk (hazard ratio 23, 95% confidence interval 13-42), with a median time-to-recurrence of 6

months and time-to-death of 11 months (versus >60 months for both outcomes among low-risk patients; p<0.001).

In this study, we evaluated the efficacy of various treatment regimens compared to surgery alone (S) in patients stratified into high vs low mortality risk categories. To gain better understanding, we compared the difference in the median time-to-recurrence and death between various treatment regimens in patients sub-stratified into four risk categories. The treatments considered include surgery with neck dissection (S+ND), surgery with irradiation (S+IR) and surgery with ND and IR (S+ND/IR). The functional analysis of the molecular pathways common to prognostic miRNAs were also conducted.

MATERIALS AND METHODS

Subjects and Study Design

Following approval from the Institutional Review Board (IRB), 836 early stage OSCC patients, ≥18 years old, newly-diagnosed with primary OSCC and with a minimum of 5-year clinical outcomes information were identified from Columbia University Irving Medical Center, Weill Cornell Medicine, University of Hawaii Cancer Research Center, the Iowa Cancer Registry at the University of Iowa, and the Eastern Division of Cooperative Human Tissue Network (CHTN). Subjects who were found to have occult lymph node metastasis following initial surgery were excluded. Subjects with the Eastern Cooperative Oncology Group (ECOG) performance-status score of 0 (no symptoms) or 1 (mild symptoms) were included.

The following clinico-demographic information was obtained from the electronic clinical record; age at diagnosis, gender, race/ethnicity (white non-Hispanic, white Hispanic, black non-Hispanic, black Hispanic, Asian), TNM stage (I vs II), histologic tumor grade (well vs moderate-to-poorly differentiated), treatment received (surgery with or without neck dissection, irradiation, or both neck dissection and irradiation), tobacco use (never/former vs

current) and alcohol abuse (4 or more drinks on any day or 8 or more drinks per week; never/former vs current). Time of initial surgical treatment until cancer recurrence and cancer-specific death were also noted.

For each subject, archived formalin-fixed paraffin-embedded (FFPE) tissue blocks were retrieved. In case the subject had recurrent and/or second primary OSCC, the initial OSCC surgical tissue sample was utilized for the analysis. Ten 10-μm sections were obtained from archived FFPE tumor tissue samples for all subjects. For each sample, a representative section was stained with H&E and reviewed by a pathologist to identify regions containing >90% malignant epithelial cells for macrodissection. Total RNA was isolated from tissues using RNeasy FFPE kits (Qiagen Inc., Valencia, CA) following the manufacturer's protocol, yield was quantitated by Nanodrop, and samples were stored at -80° C.

MicroRNA expression assessment by quantitative real-time PCR

The prognostic miRNA-127-3p, 4736, 655-3p expression levels were quantified using the miScript II Rt kit (Qiagen). Briefly, 9 μL of isolated RNA was added to the cDNA master mix, composed of 5× miScript HiSpec Buffer, 10× miScript Nucleics Mix, miScript Reverse Transcriptase Mix, and water, to a total volume of 20 μL. The cDNA was incubated at 37 °C for 60 min, followed by 5 min incubation at 95 °C and then diluted 11 times. For amplification reactions, the miScript miRNA PCR Custom Array with a miScript SYBR Green PCR kit (Qiagen) was used in a 7300 qPCR system (Applied Biosystems Inc., Beverly, MA), following the cycling conditions recommended by the supplier (15 min at 95 °C, followed by 40 cycles of 15 s at 94 °C, 30 s at 55 °C, and 30 s at 70 °C). The coefficient of variation was calculated and values <5% were considered acceptable. Test samples were assayed in duplicate with the laboratory blinded to survival status and with 5% duplication after relabeling. Data was analyzed to determine the threshold cycle (Ct). The endogenous control RUN was used to normalize the relative expression of target miRNAs (ΔCt). The samples with undetermined Ct

value for the control (RNU6-6p) were excluded from analysis. Those with an undetermined Ct for specific miRNAs were assigned a value of 39.99.

Mortality risk score calculation

Using the miRNA-based mortality risk score formula, the risk score was calculated for all subjects as previously described [7]. Briefly, we had developed the risk score formula by first performing the univariate analysis for all covariates including age, gender, race, TNM stage, depth of invasion, close/positive surgical margins, perineural invasion, histologic grade and the expression levels of selected miRNAs. To develop the best prognostic model, we repeated the cross-validation procedure 1,000 times. We further considered variables that were included in the backward-stepwise selection Cox model on time-to-death with p-value<0.1 more than 10% of the times out of the 1,000 cross-validations. Different Cox models with different sets of selected variables were constructed and the c-indexes calculated. The model with the best performance (highest c-index) was selected as the final prognostic model. Using the multiple logistic regression model, we constructed a receiver-operating characteristic (ROC) curve and calculated the area under the curve (AUC) for the test and the validation cohorts.

We then calculated the mortality risk score by summing the expression values of the selected miRNAs and covariates weighted by the regression coefficients obtained from the multivariate Cox regression analyses. **Mortality risk score** = (-0.7 x expression value of miRNA-127-3p) + (-0.3 x expression value of miRNA-4736) + (0.1 x expression value of miRNA-655-3p) + (0.9 x 0 for TNM Stage I; 1 for TNM Stage II) + (0.4 x 0 for well-differentiated; 1 for moderately/poorly differentiated), in which miRNA expression level is the ΔCt value of each miRNA. Based on the individual mortality risk scores, the patients were first stratified into high ($\geq$0) vs low (<0) mortality risk groups, and then further stratified into highest ($\geq$2), moderately-high (<2-1), moderately-low (<1-0) and low (<0) risk groups.

Prognostic miRNA functional analysis

Network visualization and functional analysis were previously performed using Cytoscape v3.2.0 to identify potential gene targets of miRNA-127-3p, 4736, 655-3p [7]. We used the gene targets from the previous study to identify the intersection among genes that control cancer recurrence and aggressiveness and the three miRNAs targets. Venn diagram was constructed to visualize gene targets common to three miRNAs.

Statistical analysis

We calculated the individual mortality risk scores for all patients in the four treatment groups using our miRNA-based mortality risk score formula. Based on these mortality risk scores, the patients were stratified into high (≥0) vs low (<0) mortality risk groups. For each risk group, the median time to death and the median time to recurrence, as well as the 5-year survival rate was assessed. The hazard ratios (HR) of the treatments S+ND, S+IR, S+ND/IR was computed over surgery only. The Kaplan-Meier curves were generated for the high and low-risk strata of the four treatment groups. Statistical analyses were conducted using R.

RESULTS

Subject characteristics

The demographic and clinico-pathologic characteristics of each treatment category is shown in **Table 1** (total n=836). The treatment groups include surgery only (S; n=551), surgery with neck dissection (S+ND; n=164), surgery with radiotherapy (S+IR; n=76) and surgery with neck dissection and irradiation (S+ND/IR; n=45). Compared to S only group, significantly more patients with higher TNM stage (Stage II) and the histologic tumor grade (moderately/poorly-differentiated carcinoma) received treatment additional to surgery.

Mortality risk score-based stratification

The miRNA-based mortality risk score formula was utilized to calculate the risk score for all patients. Within each treatment category, the patients were stratified into either high-

risk (≥0) vs low-risk (<0). The median time-to-recurrence and time-to-death, as well as 5-year survival rates were calculated for high vs low risk strata in each treatment category (**Table 2**). Within the high-risk group, S+ND significantly improved the 5-year survival (75%) over surgery only (46%). In contrast, IR in addition to surgery did not contribute to improved survival (5-year survival rate for S+IR of 44% and S+ND+IR of 62%) as shown in **Figure 1a**. The hazard ratio (HR) of S+ND over S was 0.37 (95% CI: 0.2-0.6) with a p-value of 0.0005, indicating a survival benefit for those with a high mortality risk score.

In the low-risk group, S alone was associated with the highest 5-year survival rate compared to other treatment modalities (Table 2). S+ND that demonstrated significant survival benefit in the high-risk group, was associated with lower 5-year survival of 74% compared to S only (5-year survival rate of 89%) in the low-risk group. Moreover, other treatment modalities significantly decreased survival in the low-risk group compared to S only. The HR of S+ND over S was 2.6 (95% CI: 1.6-4.2), for S+IR 6.5 (95% CI: 3.9-10.8) and for S+ ND/IR 3.4 (95% CI: 1.7-6.7) all with p-values ≤0.0001. Thus, for the low mortality risk group, surgery only was the best treatment option (**Figure 1b**).

Sub risk-strata analysis of S alone and S+ND treatment groups

For the patients who were treated with S or S+ND, we compared the median time-to-recurrence, the time-to-death and 5-year survival rate by sub-stratifying risk categories to highest (≥2), moderately-high (<2-1), moderately-low (<1-0) and low (<0) as shown in **Table 3**. In the S only group, those with risk score of ≥1 demonstrate significantly shorter median time-to-recurrence (10 months) and, subsequently, a median time-to-death of 17 months. For the S+ND treatment group, 27% (14 out of 52) with a risk score of 1 or higher had cancer-specific deaths. This subgroup of patients had very high risk score with a median risk score of 6 (range: 3-10). The median time-to-recurrence was 9.5 months, while the median time-to-death was 14.5 months.

Functional analysis of prognostic miRNAs

We identified common gene targets of miRNA-127-3p, 4736, 655-3p and selected the ones associated with cancer recurrence and aggressiveness (**Figure 2**). The Rac family small GTPase 1 (Rac1) was identified as a common target of three miRNAs. We also identified Rho GTPases activated p21-activated kinases (PAKs) pathway, including Cdc42 and hTERT as key targets common to three miRNAs. Rho GTPases are crucial regulators of cell migration and are altered in many cancer types, including colon, glioblastoma and head and neck cancer [15]. Rac, Rho and Cdc42 are subfamilies of Rho GTPase [16]. Integrin-mediated cell-extracellular matrix adhesion activates Rac1, which directly binds and activates PAKs and other effectors including phosphatidylinositol-4-phosphate 5-kinase, Nap125, PIR121 and IRSp53, resulting in increased membrane protrusions and actin polymerization [16,17]. The other member of Rho GTPase subfamily Cdc42, once activated, phosphorylates PAK1 and PAK2, which in turn leads to filopodia formation [17]. These changes either by themselves or integrated can affect gene expression, cell cycle progression and apoptosis [17]. Importantly, Cdc42/Rac1 participates in the post-transcriptional control of telomerase activity by transcriptional upregulation of human telomerase reverse transcriptase, hTERT [18,19]. Hence PAKs-Cdc42/Rac1-hTERT pathway plays a central role in cancer recurrence and aggressiveness and are targeted by the prognostic miRNAs.

hTERT expression analyses

To assess hTERT overexpression in more aggressive form of OSCC, we performed quantitative immunofluorescent assays in ten cancer cases from the S+ND treatment group with risk scores of 1 or higher who had cancer recurrence. The formalin-fixed paraffin-embedded tissue slides were stained with anti-human hTERT (Rockland Immunochemicals, Limerick, PA). The hTERT stain concentration and the number of nuclei staining with hTERT were quantified using a macro derived from the Leica Quantitative Algorithm v1. The hTERT stain concentration was multiplied by the number of hTERT-expressing tumor cells to obtain

final hTERT expression levels. After adjusting for the outliers, we had eight evaluable cases. Differential hTERT expression levels were compared between those who had cancer-specific death following recurrence (n=4) vs those who had 5-year survival despite having a recurrence (n=4) (**Figure 3a**). hTERT level was 2.4-fold higher in those who had a cancer-specific death (an average hTERT expression level of 8,061; an average hTERT stain concentration of 3.8, with an average of 2,318 hTERT-expressing tumor cells) compared to those with 5-year survival (an average hTERT expression level of 3,330; an average hTERT stain concentration of 3.5, with an average of 884 hTERT-expressing tumor cells). Due to the small sample size, statistical significance could not be assessed. hTERT level correlated with the mortality risk scores, demonstrating that elevated hTERT level is associated with poor survival.

We also assessed feasibility of hTERT level quantification in the patient-derived normal and OSCC organoids. We first obtained small piece (5x5x3mm) of normal and OSCC tissue from patients at the time of surgery. Surface epithelium from normal tissues and OSCC tumor islands within lamina propria were isolated. Tissue sections were minced, enzymatically dissociated, and forced through a 70 μm cell strainer. The single cell suspension (4×10^5/ml) was mixed with Matrigel (Corning, Corning, NY) and 2×10^4 cells in 50 μl of Matrigel were seeded into the 24-well plates. Organoids were grown for 10-14 days at 37°C in a humidified atmosphere of 5% CO_2 as previously described [19]. Under an inverted phase-contrast microscope, growing organoids were observed and photomicrographed to determine their number and size. Organoid formation rate was defined as the average number of $\geq$50 μm spherical structures at day 14 that was divided by the total number of cells seeded in each well at day 0. Organoids were recovered and fixed overnight in paraformaldehyde for histological examination and hTERT quantitative immunofluorescent

assay. There was minimal hTERT immunofluorescent staining in normal organoids and stronger immunofluorescent staining in OSCC organoids (**Figure 3b**).

DISCUSSION

Currently there is no clinical modality to identify patients at high-risk for cancer-specific death among those assigned to early-stage OSCC (TNM stages I & II). Because 80% of oral cancer patients are in early-stage at the time of diagnosis [2], a window of opportunity exists in which proper prognostication and subsequent decisions for additional treatment can dramatically improve the 5-year survival of patients with this deadly disease.

Using the miRNA-based mortality risk score formula, we assigned a risk score to all patients and assessed the survival benefit in high ($\geq$0) vs low (<0) risk strata based on the treatment received. Compared to S only, S+ND significantly increased the median time-to-recurrence from 26 months to $\geq$60 months and the 5-year survival rate from 46% to 75% ($p<0.001$) for the high-risk group, consistent with other reports that S+ND is associated with survival benefit in early-stage OSCC [20,21]. Improved 5-year survival in the S+ND group was most likely secondary to prolonged time-to-recurrence. Indeed, initial treatment modality and time-to-recurrence were reported to be independent prognostic variables [22].

Paradoxically, the patients in the low mortality risk group who received S+ND had a lower 5-year survival rate of 74% compared to 89% in the S only group. The significant reduction in the 5-year survival in the low-risk strata who had S+ND may be explained by the low success rate of salvage surgery at the time of cancer recurrence [22,23]. With initial S+ND treatment, patients experienced recurrence in a less predictable fashion, often in the contralateral neck [22,23]. In contrast, patients treated with S only were more likely to present with nodal disease confined to the neck at levels I, II, and III, which were successfully removed during salvage surgery [22,23]. Similarly, in the high-risk strata treated by S+ND, 54% of those with cancer recurrence died due to failed salvage surgery. S+IR and S+IR+ND demonstrated minimal survival benefit over S or S+ND for both high and low risk strata.

From the subgroup analysis of those treated with S+ND and with higher risk scores (≥1), we identified a subset of individuals with distinctly aggressive tumors characterized by high-risk scores ranging from 3-10, a median time-to-recurrence of 9.5 months and a median time-to-death of 14.5 months. Based on our study, it may be beneficial for patients to be risk stratified using the prognostic marker at the time of biopsy. For those with low mortality risk scores (<0), surgery only without neck dissection is the most beneficial treatment modality. On the other hand, for those with high-risk scores (≥0), S+ND will greatly improve the 5-year survival rate. However, regardless of treatment selected, those with risk score of ≥1 may benefit from additional therapy to prevent recurrences, which will further improve the 5-survival rate.

Based on the functional analysis of the prognostic miRNAs, hTERT along with few other molecules in the same signaling pathway were demonstrated to be targeted by all three miRNAs. Telomerase shortening at every replication cycle limits the life span of human somatic cells. In contrast, activation of telomerase is an essential step in cancer cell immortalization. Telomerase reverse transcriptase (TERT or hTERT in humans) is a catalytic subunit of the enzyme telomerase [24]. Upregulation of hTERT is the key mechanism in which cancer cells maintain their telomer length, thereby acquiring the ability to escape senescence [24]. In head and neck cancer, 85% of cancers acquire the capability to replicate indefinitely through the reactivation of hTERT [25]. A substantial body of studies have uncovered novel extra-telomeric non-canonical functions of hTERT, many of which affect cellular processes including signaling pathways for the regulation of cell survival, resistance to stress, and apoptosis [26]. Importantly, through the interaction of hTERT with the Wnt/β-catenin and NF-kB signaling pathways, the expression of telomerase may affect cancer invasiveness and metastasis [27-29]. Thus, elevated levels of hTERT in cancer cells may influence the response to treatment as well as cancer progression and metastasis, making it a potentially attractive drug target and also a marker of drug response. In fact, high hTERT

levels in head and neck cancer were independently associated with worse response to therapy, regional failure, progression, and death [25].

Our quantitative immunofluorescence study demonstrated elevated levels of hTERT in high-risk OSCC patients who had cancer recurrence and death, compared to those who survived despite having cancer relapse. In patient-derived organoids, we showed that there is overexpression of hTERT in OSCC and minimal expression in normal organoids. Others have reported similar findings. Elevated expression of hTERT was associated with a poor prognosis in solid tumors such as gastric, lung, cervical, head and neck, breast, and ovarian cancer as well as glioblastoma [30,31]. In head and neck cancer patients, elevated hTERT expression was associated with higher recurrence rate ($p = 0.044$) and a lower 5-year survival rate ($p = 0.011$) [33]. An elevated level of hTERT was also observed in oral cells within the cancerized field [34]. Moreover, hTERT expression level correlated with degree of oral preneoplasia [33]. Compared to normal oral mucosa, hTERT expression was elevated by 6.9-fold in OSCC [33].

Three-dimensional (3D) tumor organoid models have been consistently shown to faithfully recapitulate features of the tumor of origin in terms of cell differentiation, heterogeneity, histoarchitecture and clinical drug response [35-38]. Thus, there is increasing interest in developing tumor organoid models for drug development and personalized medicine applications. Functional precision therapy approaches where the primary tumor tissue is directly exposed to drugs to determine efficacy have the potential to boost personalized medicine efforts and influence clinical decisions [39-42]. A recent study found that patient-derived organoids could accurately predict patient responses to therapy, with 100% sensitivity and 93% specificity [43]. While establishing patient-derived xenografts is costly and time-consuming, *in vitro* 3D organoids derived from primary cancers can be established rapidly, with successful passage within 10-14 days of *in vitro* growth and with >80% efficiency [35]. Thus far, we have cultivated patient-derived organoids from normal oral

epithelium and OSCC. These organoids can be utilized in future as a functional *in vitro* testing platform to explore novel therapeutic options, such as the hTERT antagonist.

CONCLUSION

In response to the critical need to subdivide traditional tumor classes into subsets that behave differently and also to refine and improve prognostication and treatment selection, we have developed and validated a novel miRNA-based prognostic model to predict survival outcome in patients who are already categorized into 'early-stage' by the TNM system. For clinical practicality, we developed a parsimonious risk score formula that is capable of translating miRNA expression levels assessed by qRT-PCR at the time of initial cancer diagnosis into a score that reflects the risk of cancer-specific mortality during the 5-year period from the time of surgery. Improved survival was observed in high-risk strata with S+ND treatment and in low-risk strata with S only. Moreover, we demonstrated that those with higher risk score of ≥ 1 may benefit from therapeutic intervention in addition to surgical treatment.

Based on functional analysis of the prognostic miRNAs, we discovered that hTERT is associated with high mortality risk scores, and shorter median time-to-recurrence and death. Thus, hTERT is a promising drug target and the hTERT inhibitor has potential utility as a chemopreventive/therapeutic agent. We plan to take an innovative approach linking prognostic marker-based mortality risk assessment with appropriate risk-adjusted therapy to improve overall survival. We have begun to establish a functional platform for the patient-derived organoid-based drug testing, which has a potential role in clinical decision-making tailored to each individual. Assessment of hTERT antagonists will require testing in mouse models as well as in clinical trials, which we plan to conduct as the next step.

Data Availability

The data provided in this publication will be available from the corresponding author upon request.

Conflicts of Interest

The authors declare that they have no conflicts of interest regarding the publication of this paper.

Funding Statement

This work was supported by the NIH/NIDCR R01DE026801 (A. Yoon), the NIH/NIEHS P30ES009089 and the NIH/NCI P30CA013696 (Columbia University).

Acknowledgements

We thank Charis Yoon for her assistance in data organization, and Qiao Wang for her technical assistance.

REFERENCES

1. Rivera C. Essentials of oral cancer. Int J Clin Exp Pathol 2015;8:11884-11894.
2. Sasahira T, Kirita T. Hallmarks of cancer-related newly prognostic factors of oral squamous cell carcinoma. Int J Mol Sci 2018;19:2413.
3. Pires FR, Ramos AB, de Oliveira JB, et al. Oral squamous cell carcinoma: clinicopathological features from 346 cases from a single Oral Pathology service during an 8-year period. J Appl Oral Sci 2013;21:460-467.
4. Weatherspoon DJ, Chattopadhyay A, Boroumand S, Garcia AI. Oral Cavity and Oropharyngeal Cancer Incidence Trends and Disparities in the United States: 2000–2010. Cancer Epidemiol 2015;39:497-504.
5. De Abre PM, Co ACG, Azevedo PL, et al. Frequency of HPV in oral cavity squamous cell carcinoma. BMC Cancer 2018;18:324.
6. Lydiatt WM, Patel SG, O'Sullivan B, et al. Head and neck cancers-major changes in the American Joint Committee on cancer eighth edition cancer staging manual. CA Cancer J Clin 2017;67:122-137.
7. Yoon AJ, Wang S, Wang T, Kutler DI, LaRoche D, Philipone E, Peters SM, Hernandez B, McDowell BD, Stewart CR, Momen-Heravi F, Santella RM. MicroRNA-based risk scoring system to identify early-stage oral squamous cell carcinoma patients at high-risk for cancer-specific mortality. Head Neck 2020. doi.org/10.1002/hed.26089.
8. Gombos K, Horvath R, Szele E, et al. miRNA expression profiles of oral squamous cell carcinomas. Anticancer Res 2013;33:1511-1517.
9. Troiano G, Mastrangelo F, Caponio VCA, et al. Predictive prognostic value of tissue-based microRNA expression in oral squamous cell carcinoma: a systemic review and meta-analysis. J Dent Res 2018;97:759-766.
10. Sarode GS, Sarode SC, Maniyar N, Anand R, Patil S. Oral cancer database: a comprehensive review. J Oral Pathol Med 2018;47:547-556.

11. Myers J. Potential role of micro-RNAs in head and neck tumorigenesis. Head Neck 2010;32:1099-1011.
12. Manikandan M, Deva Magendhra Rao AK, Arunkumar G, et al. Oral squamous cell carcinoma: microRNA expression profiling and integrative analyses for elucidation of tumourigenesis mechanism. Mol Cancer. 2016;15:28.
13. Ramdas L, Giri U, Ashorn CL, Coombes KR, El-Naggar A, Ang KK, Story MD. MiRNA expression profiles in head and neck squamous cell carcinoma and adjacent normal tissue. Head Neck 2009;31:642–654.
14. Kumarasamy C, Madjav MR, Sabarimurugan S, et al. Prognostic value of miRNAs in head and neck cancers: a comprehensive systemic and meta-analysis. Cells 2019;8. doi: 10.3390/cells8080772.
15. Lin Y and Zheng Y. Approaches of targeting Rho GTPases in cancer drug discovery. Expert Opin Drug Discov 2015;10:991-1010. Kirkpatrick KL, Mokbel K. The significance of human telomerase reverse transcriptase (hTERT) in cancer. EJSO 2001;27:754-760.
16. Cardama GA, Gonzalez N, Maggio J, Menna PL, Gomez DE. Rho GTPase as therapeutic targets in cancer. Int J Oncol 2017;51:1025-1034.
17. Sahai E and Marshall CJ. RHO-GTPases and cancer. Nat Rev Cancer 2002;2:133-142.
18. Gomez DLM, Armando RG, Cerrudo CS, Ghiringhelli PD and Gomez DE. Telomerase as a cancer target. Development of new molecules. Curr Top Med Chem 2016;16:2432-2440.
19. Karakasheva T, Kijimma T, Shimononosono M, et al. Generation and characterization of patient-derived head and neck, oral, and esophageal cancer organoids. Curr Protoc Stem Cell Biol 2020. doi.org/10.1002/cpsc.109.
20. Mirea D, Grigore R, Safta D, Mirea L, Popescu CR, Popescu B, Bertesteanu SVG. Elective neck dissection in patients with stage T1-T2N0 carcionma of the anterior tongue. Hippokratia 2014;18:120-124.

21. Mizrachi A, Migiliacci JC, Montero PH, McBride S, Shah JP, Patel SG, Ganly I. Neck recurrence in clinically node-negative oral cancer: 27-year experience at a single institution. Oral Oncol 2018;78:94-101.
22. Kernohan MD, Clark JR, Gao K, Ebrahimi A, Milross CG. Predicting the Prognosis of Oral Squamous Cell Carcinoma After First Recurrence. Arch Otolaryngo Head Neck Surg 2010;136:1235-1239.
23. Kowalski LP. Results of salvage treatment of the neck in patients with oral cancer. Arch Otolaryngol Head Neck Surg 2002;128:58-62.
24. Leao R, Apolonio JD, Lee D, Figueiredo A, Tabori U, Castelo-Branco P. Mechanisms of human telomerase reverse transcriptase (hTERT) regulation: clinical impacts in cancer. J Biomed Sci 2018;25:22.
25. Boscolo-Rizzo P, Rampazzo E, Polesel J, et al. Predictive and prognostic significance of telomerase levels/telomere length in tissues and peripheral blood in head and neck squamous cell carcinoma. Sci Rep 2019. doi.org/10.1038/s41598-019-54028-x.
26. Saretzki G. Extra-telomeric functions of human telomerase: cancer, mitochondria and oxidative stress. Curr. Pharm. Des 2014;20:6386-6403.
27. Boscolo-Rizzo P, et al. Telomeres and telomerase in head and neck squamous cell carcinoma: from pathogenesis to clinical implications. Cancer Metastasis Re. 2016;35:457-474.
28. Li Y, Tergaonkar V. Noncanonical functions of telomerase: implications in telomerase-targeted cancer therapies. Cancer Res 2014;74:1639-1644.
29. Wu Y, et al. Telomerase reverse transcriptase mediates EMT through NF-κB signaling in tongue squamous cell carcinoma. Oncotarget 2017;8:85492-85503.
30. Wang K, Wang RL, Liu JJ, et al. The prognostic significance of hTERT overexpression in cancers: a systemic review and meta-analysis. Medicine 2018;98:e11794.

31. Kirkpatrick KL, Mokbel K. The significance of human telomerase reverse transcriptase (hTERT) in cancer. EJSO 2001;27:754-760.

32. Che HH, Yu CH, Wang JT, et al. Expression of human telomerase reverse transcriptase (hTERT) protein is significantly associated with the progression, recurrence and prognosis of oral squamous cell carcinoma in Taiwan. Oral Oncol 2007;43:122-129.

33. Kim HR, Chistensen R, Park NH, Sapp P, Kang MK, Park NH. Elevated expression of hTERT is associated with dysplastic cell transformation during human oral carcinogenesis in situ. Clin Cancer Res 2001;7:3079-3086.

34. Fabricius EM, Gurr U, Wildner GP. Telomerase activity levels in the surgical margin and tumour distant tissue of the squamous cell carcinoma of the head-and-neck. Anal Cell Pathol 2002;24:25-39.

35. Karakasheva T, Kijimma T, Shimononosono M, et al. Generation and characterization of patient-derived head and neck, oral, and esophageal cancer organoids. Curr Protoc Stem Cell Biol 2020. doi.org/10.1002/cpsc.109.

36. Driehuis E, Kolders S, Spelier S, Lõhmussaar K, Willems SM, Devriese LA, et al. Oral mucosal organoids as a potential platform for personalized cancer therapy. Cancer Discov 2019;9:852-871.

37. Kijima T, Nakagawa H, Shimonosono M, et al. Three-Dimensional Organoids Reveal Therapy Resistance of Esophageal and Oropharyngeal Squamous Cell Carcinoma Cells. Cell Mol Gastroenterol Hepatol. 2019;7:73-91.

38. Phan N, Hong JJ, Tofig B, et al. A simple high-throughput approach identifies actionable drug sensitivities in patient-derived tumor organoids. Commun Biol 2019. doi.org/10.1038/s42003-019-0305-x.

39. Cummings CA, Peters E, Lacroix L, Andre F, Lackner MR. The role of next-generation sequencing in enabling personalized oncology therapy. Clin Transl Sci 2016;9:283-292.

40. Simon R, Roychowdhury S. Implementing personalized cancer genomics in clinical trials. Nat Rev Drug Discov 2013;12:358-369.

41. Letai A. Functional precision cancer medicine-moving beyond pure genomics. Nat Med 2017;23:1028-1035.

42. Vlachogiannis G et al. Patient-derived organoids model treatment response of metastatic gastrointestinal cancers. Science 2018;359:920-926.

43. Gartrell RD, Marks DK, Hart TD, Li G, Davari DR, Wu A, Blake Z, Lu Y, Askin KN, et al. Quantitative analysis of immune infiltrates in primary melanoma. Cancer Immunol Res 2018;6:481-493.

Table 1. Clinical and pathologic characteristics of the early-stage oral squamous cell carcinoma patients included in this study.

	S Only	S+ND	S+IR	S+ND/IR
Patients	n=551	n=164	n=76	n=45
Age				
Mean (range)	66 (21-97)	61 (25-87)	65 (24-90)	58 (35-80)
Gender				
Female	218 (40%)	84 (51%)	24 (32%)	21 (47%)
Male	333 (60%)	80 (49%)	52 (68%)	24 (53%)
Race/Ethnicity				
White non-Hispanic	383 (70%)	92 (56%)	30 (39%)	22 (49%)
White Hispanic	80 (15%)	15 (9%)	9 (12%)	9 (20%)
Black non-Hispanic	22 (4%)	4 (2%)	1 (1%)	7 (6%)
Black Hispanic	5 (1%)	0 (0%)	0 (0%)	0 (0%)
Asian	52 (9%)	34 (21%)	27 (36%)	5 (11%)
Unknown	9 (2%)	19 (12%)	9 (12%)	2 (4%)
TNM Stage				
Stage I	428 (78%)	81 (49%)	40 (53%)	17 (38%)
Stage II	123 (22%)	83 (51%)	36 (47%)	28 (62%)
Histologic Grading				
Well-differentiated	291 (53%)	76 (46%)	29 (38%)	8 (18%)
Moderately/Poorly-differentiated	260 (47%)	88 (54%)	47 (62%)	37 (82%)
Smoking Status				
Never	163 (30%)	64 (39%)	2 (3%)	17 (38%)
Past	72 (13%)	39 (24%)	9 (12%)	7 (16%)
Current	54 (48%)	12 (7%)	5 (7%)	6 (13%)
Unknown	262 (48%)	49 (30%)	60 (79%)	15 (33%)
Alcohol Abuse				
Never	201 (36%)	80 (49%)	4 (5%)	22 (49%)
Past	32 (6%)	14 (9%)	6 (8%)	0 (0%)
Current	56 (10%)	21 (13%)	6 (8%)	8 (18%)
Unknown	262 (48%)	49 (30%)	60 (79%)	15 (33%)

Table 2. The efficacy of various treatment regimens in oral squamous cell carcinoma patients stratified into high (risk score ≥0) and low-risk (risk score <0) categories using the microRNA-based prognostic model; surgery (S) only, surgery with neck dissection (S+ND), surgery with irradiation (S+IR) and surgery with neck dissection and irradiation (S+ND/IR).

Treatment	Risk Category	Median Time-to-Death	Median Time-to-recurrence	Cancer Death	5-year Survival
Surgery only	High risk (>0)	50	26	54%	46%
	Low risk (<0)	≥60	≥60	11%	89%
S + ND	High risk	≥60	≥60	25%	75%*
	Low risk	≥60	≥60	26%	74%*
S + IR	High risk	43	41	56%	44%
	Low risk	≥60	33	49%	51%*
S + ND/IR	High risk	≥60	7	38%	62%
	Low risk	≥60	≥60	34%	66%*

*p≤0.05 when compared with the same risk strata of S only.

Figure 1a. Kaplan-Meier curve demonstrating survival benefit of surgery with neck dissection over other treatment modalities in oral squamous cell carcinoma patients with high mortality risk score (≥0).

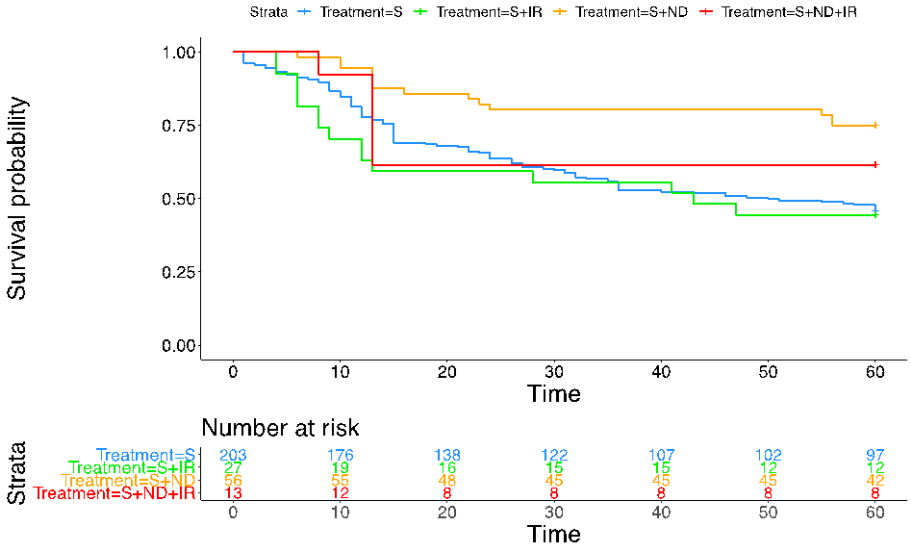

Figure 1b. Kaplan-Meier curve delineating survival benefit of surgery only over other treatment modalities in oral squamous cell carcinoma patients with low mortality risk score (<0).

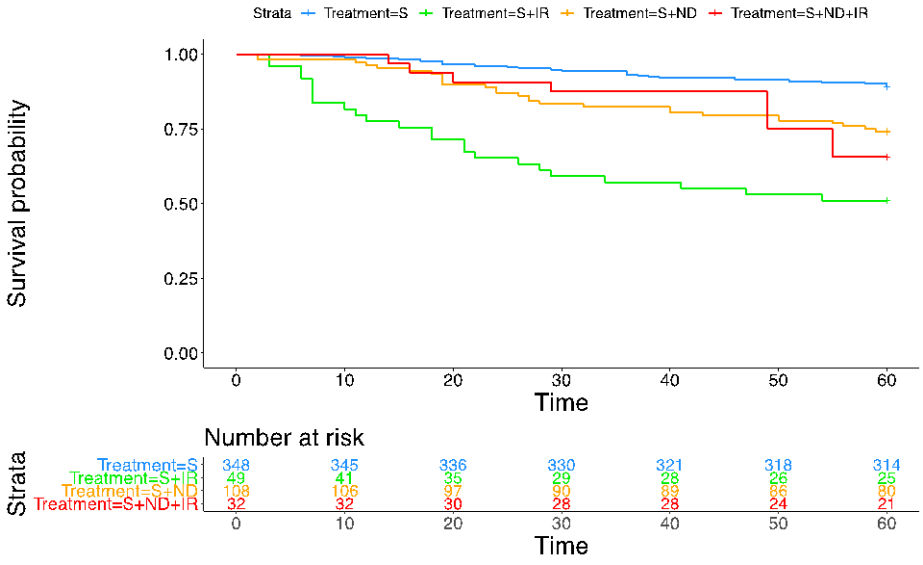

Table 3. The median time-to-recurrence, time-to-death and survival rate in oral squamous cell carcinoma patients treated with surgery only (S) or surgery with neck dissection (S+ND). Initial stratification into high versus low risk, and then sub-risk stratification into highest, moderately-high, moderately-low and low risks are shown. The 'higher risk (≥1)' strata represents a group of patients at greater risk of cancer relapse and death, compared to 'lower risk (<1) strata' regardless of treatment received (S or S+ND).

Risk Strata	Sub-Risk Strata	Risk Scores	Median Time-to-Death	Median Time-to-Recurrence	Cancer Death	5-year Survival	Clinical Risks
High-risk	**Highest risk**	**≥2**					Higher Risk
	S only		11 (months)	6 (months)	94%	6%	
	S+ND		≥60	58	32%	68%	
	Moderately-high risk	**1 to <2**					
	S only		22	14	71%	29%	
	S+ND		≥60	≥60	0%	100%	
	Moderately-low risk	**0 to <1**					Lower Risk
	S only		≥60	46	42%	58%	
	S+ND		≥60	≥60	0%	100%	
Low-risk	**Low risk**	**<0**					
	S only		≥60	≥60	11%	89%	
	S+ND		≥60	≥60	26%	74%	

Figure 2. Common gene targets of miRNA-127-3p, 4736, 655-3p that are associated with cancer recurrence and aggressiveness. **a**. Visualization of the gene targets. Cancer-related pathways involving Rac family small GTPase 1 (Rac1), p21-activated kinases (PAKs), Cdc42, and human telomerase reverse transcriptase (hTERT) were identified in association with three microRNAs. **b**. Venn diagram showing common gene targets.

Figure 2a. Gene targets.

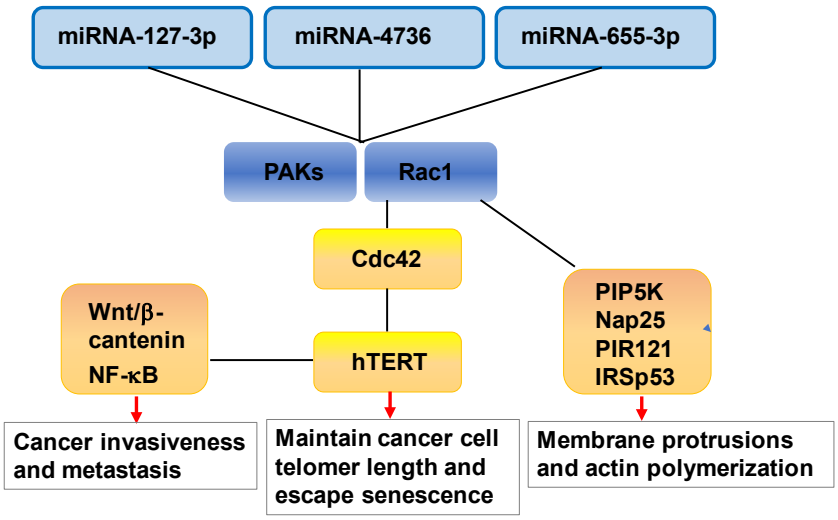

Figure 2b. Venn diagram.

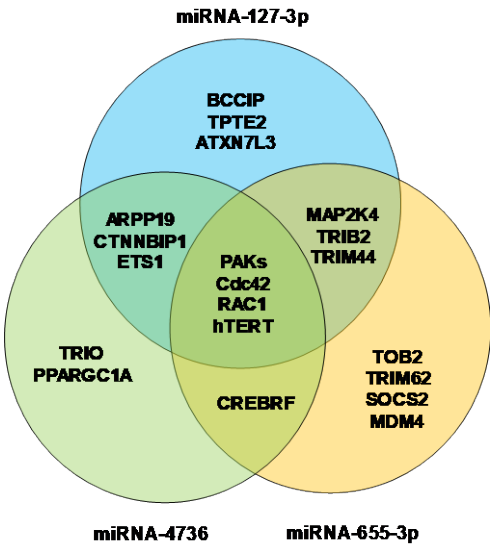

Figure 3. The expression levels of hTERT assessed by quantitative immunofluorescence assay.

Figure 3a. Elevated hTERT (bright red dots on blue DAPI-stained nuclei) in OSCC associated with poor prognosis (cancer recurrence and death within 5-year period) compared to those who survived the 5-year period despite cancer recurrence, in the surgery with neck dissection (S+ND) treatment group with higher mortality risk scores (≥1). Dot plots comparing hTERT expression levels in two groups. Bars indicate the mean hTERT expression.

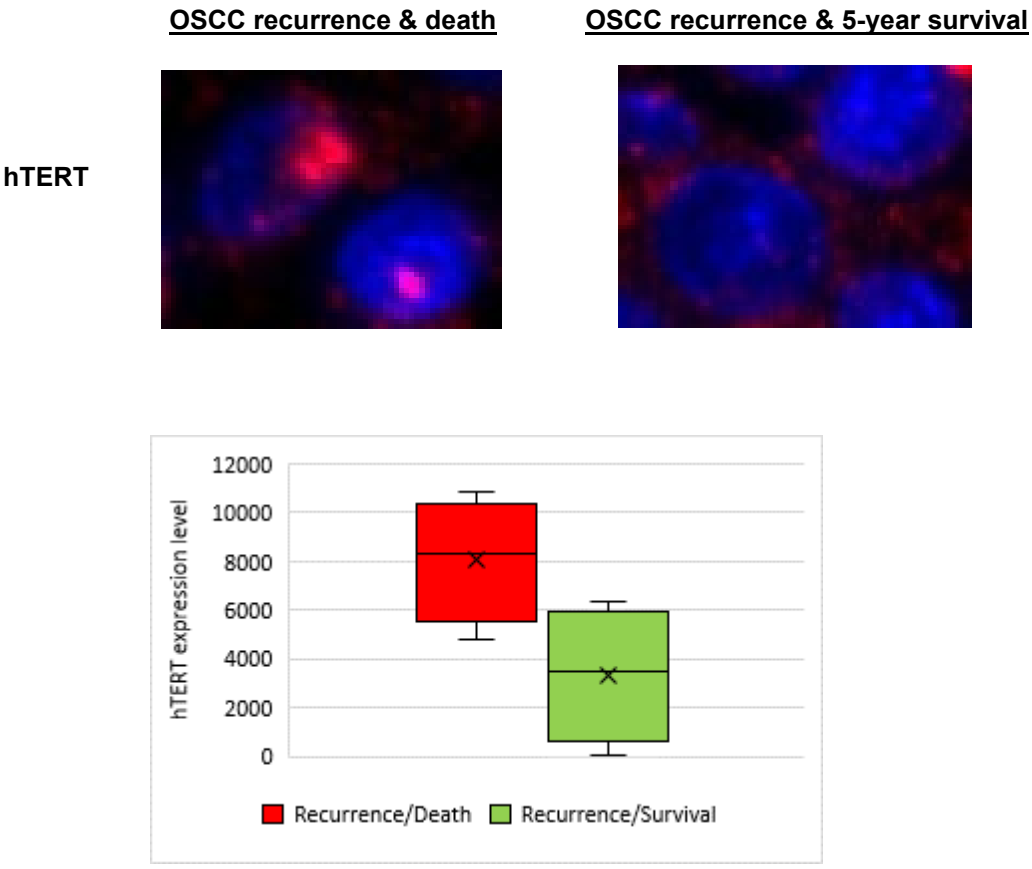

Figure 3b. H&E of normal and OSCC organoids. Minimal hTERT expression is observed in normal oral organoids, in comparison with the higher hTERT expression (bright red nuclear and peri-nuclear dots) in OSCC organoids.